Imaging Single Cardiac Ryanodine Receptor Ca^{2+} Fluxes in Lipid Bilayers

S. Peng,* N. G. Publicover,† G. J. Kargacin,‡ D. Duan,* J. A. Airey,* and John L. Sutko*
*Department of Pharmacology and the †Biomedical Engineering Program, University of Nevada, Reno, Nevada; and ‡Department of Physiology and Biophysics, University of Calgary, Calgary, Alberta T2N 4N1, Canada

ABSTRACT In this and an accompanying report we describe two steps, single-channel imaging and channel immobilization, necessary for using optical imaging to analyze the function of ryanodine receptor (RyR) channels reconstituted in lipid bilayers. An optical bilayer system capable of laser scanning confocal imaging of fluo-3 fluorescence due to Ca^{2+} flux through single RyR2 channels and simultaneous recording of single channel currents was developed. A voltage command protocol was devised in which the amplitude, time course, shape, and hence the quantity of Ca^{2+} flux through a single RyR2 channel is controlled solely by the voltage imposed across the bilayer. Using this system, the voltage command protocol, and concentrations of Ca^{2+} (25–50 mM) that result in saturating RyR2 Ca^{2+} currents, proportional fluo-3 fluorescence was recorded simultaneously with Ca^{2+} currents having amplitudes of 0.25–14 pA. Ca^{2+} sparks, similar to those obtained with conventional microscope-based laser scanning confocal systems, were imaged in mouse ventricular cardiomyocytes using the optical bilayer system. The utility of the optical bilayer for systematic investigation of how cellular factors extrinsic to the RyR2 channel, such as Ca^{2+} buffers and diffusion, alter fluo-3 fluorescent responses to RyR2 Ca^{2+} currents, and for addressing other current research questions is discussed.

INTRODUCTION

Fluorescence measurements provide a valuable tool for analysis of the function of ion channels and transport proteins in cells, tissues, and in vitro at the single protein level. Fluorescence imaging has been particularly useful at the cell and tissue level for investigations of the activity of Ca^{2+} channels, such as ryanodine receptors (RyR) and inositol tris-phosphate receptors (IP_3R), localized to intracellular membranes and therefore inaccessible by conventional microelectrode techniques. For example, identification of local sarcoplasmic reticulum (SR) Ca^{2+} release events, Ca^{2+} sparks (Cheng et al., 1993), has provided a noninvasive experimental approach for assessing RyR channel function in intact cells. At the protein level, site-directed incorporation of fluorescent reporter molecules has been used to probe changes in the structure of transporters, such as the lactose permease in *Escherichia coli* (Vazquez-Ibar et al., 2002), and ion channels, such as the Shaker K^+ channel (Cha et al., 1999; Sonnleitner et al., 2002), that underlie the function of these proteins.

Our goal was to develop an experimental system for applying optical imaging techniques to investigations of RyR channel properties in vitro. As a consequence of their localization to intracellular membranes, RyR channels have been studied after reconstitution of membrane vesicles or purified protein in planar lipid bilayers (Fill and Copello, 2002; Sitsapesan and Williams, 1990; Smith et al., 1986; Williams et al., 2001). To take advantage of the ability of the bilayer system to measure Ca^{2+} flux through single RyR channels in a very accurate manner, we sought to develop an optical bilayer system permitting simultaneous imaging of RyR channel-related functions and recording of single channel currents.

Our work was motivated by several experimental objectives. First, analyses of events involved in activation of muscle cells and, in particular, of RyR channel function in intact cells require quantitative information about the Ca^{2+} flux underlying the imaged Ca^{2+} spark. However, extraction of this information is complicated by factors and conditions extrinsic to the RyR channel that prevent the imaged spark waveform from faithfully tracking the waveform of the underlying Ca^{2+} release flux. These factors include binding of Ca^{2+} to fixed and mobile buffers, diffusion of free Ca^{2+} and of Ca^{2+} bound to buffers and to the Ca^{2+} indicator, and binding of the Ca^{2+} indicator to cellular proteins. There is also uncertainty about the distance of the plane of focus from sites of Ca^{2+} release during imaging, and the affinity of the indicator for Ca^{2+}. The kinetics of the indicator-Ca^{2+} binding reaction may also distort the spark signal. Influences by these factors alter the response by the Ca^{2+} indicator to the Ca^{2+} flux waveform in both time and space. Defining the influences of many of these extrinsic factors in cells is problematic, because their effects can be interactive and it is difficult to perturb only a single factor in an intact cell in a controlled and systematic manner. To approach this problem, models and simulations have been used to estimate influences exerted by extrinsic factors (Baylor et al., 2002; Cannell and Soeller, 2002; Izu et al., 2001; Jiang et al., 1999; Pratusevich and Balke, 1996; Rios and Brum, 2002; Smith et al., 1998; Sobie et al., 2002). As a complementary approach to this problem, we sought to develop an experimental system in which Ca^{2+} flux through single

Submitted July 18, 2003, and accepted for publication September 4, 2003.
Address reprint requests to John Sutko, Dept. of Pharmacology, 318 Howard Bldg., Room 214, University of Nevada, Reno, NV 89557. Tel.: 775-784-4121; Fax: 775-784-1620; E-mail: sutko@unr.edu.

0006-3495/04/01/134/11 $2.00

RyR channels could be both imaged with fluorescent Ca^{2+} indicators and recorded electronically, and where the environment of the Ca^{2+} indicator could be controlled and manipulated. Such an experimental system would permit influences exerted on Ca^{2+} sparks by extrinsic factors, such as those noted above, to be investigated in a direct and systematic manner.

An optical bilayer system will also permit other aspects of RyR channel function to be studied in novel ways. For example, multiple RyR channels are thought to cluster in functional Ca^{2+} release units (CRU) (Franzini-Armstrong et al., 1999) that may activate and inactivate in a coupled manner (Copello et al., 2003; Marx et al., 1998, 2001; Ondrias and Mojzisova, 2002; Wang et al., 2002). Consistent with this notion, multiple RyR channels reconstituted in lipid bilayers from SR membranes exhibit coupled gating and both physical interactions between adjacent RyR channels and sequential activation by Ca^{2+}-induced Ca^{2+} release have been proposed as mechanisms coordinating this gating (Copello et al., 2003; Marx et al., 1998, 2001). Fluorescence imaging may provide a way to distinguish between these possibilities. There is also increasing information concerning the relationship between the primary sequence and the tertiary structure of RyR channels (Liu et al., 2002; Serysheva et al., 1999; Wagenknecht and Samso, 2002). An optical bilayer system capable of analyzing signals from fluorescent reporter molecules incorporated into RyR channels in a site-directed manner will facilitate investigations of the structure and function of this protein similar to those noted above for the lactose permease and K^+ channels. The feasibility of this approach is supported by observation of function-dependent fluorescent signals from populations of RyR channels (Ikemoto and Yamamoto, 2002; Ohkusa et al., 1991). As described in this report, as well as in an abstract (Peng et al., 2003), we have developed an optical bilayer system with the sought-after capabilities. As described in the accompanying report (Peng et al., 2004), we have utilized this system to characterize lateral diffusion by single RyR2 channels in bilayers and to identify a mechanism for preventing this movement to enhance the spatial and temporal resolutions of optical imaging related to RyR channel function.

MATERIALS AND METHODS

Materials

All salts, buffers, protease inhibitors, organic solvents, sucrose, suramin and ruthenium red were purchased from either Sigma Chemical (St. Louis, MO) or Fisher Scientific (Pittsburgh, PA) and common chemicals were of reagent grade or better. The pentaamonium salt and cell permeant AM form of fluo-3 were purchased from Molecular Probes (Eugene, OR). Phospholipids were obtained from Avanti Polar Lipids (Alabaster, AL). Chelex resin was obtained from Bio-Rad Laboratories (Hercules, CA). Halar and Kel-F polymers were obtained from Honeywell/Allied Signal (Pottsville, PA) and McMaster-Carr (Santa Fe Springs, CA), respectively.

Preparation of RyR2

Hearts were obtained from adult sheep sacrificed for other purposes at the University of Nevada farm. Sarcoplasmic reticulum membranes were isolated using differential centrifugation and sedimentation through discontinuous sucrose gradients as described previously (Airey et al., 1990; Sitsapesan and Williams, 1994). RyR2 channels were solubilized by incubating SR membranes (3 mg protein/ml) with 2% CHAPS and 1% phosphatidylcholine (PC) in a solution containing (in mM): 500 KCl, 5 DTT 20 Tris (pH 7.4) for 30 min on ice. Nonsolubilized material was removed by centrifugation at 100,000 $\times$ *g* for 30 min. Solubilized RyR channels were purified further by sedimentation through a continuous 10–30% sucrose gradient in a Beckman SW28 rotor at 24,000 $\times$ *g* for 16 h (Airey et al., 1990). Partially purified RyR channels were reconstituted into liposomes by dialysis (8 h $\times$ 4 solution changes) against 2 liters of a solution containing, in mM: 250 NaCl, 0.2 $CaCl_2$, 0.1 EGTA, 10 Mops (pH 7.4), 1 DTT. After dialysis, liposomes were pelleted by centrifugation at 266,000 $\times$ *g* for 50 min in a Beckman TL-100 rotor, resuspended in a solution containing, in mM: 500 KCl, 20 Tris/Hepes (pH 7.4), 400 sucrose, 5 DTT, rapidly frozen in liquid N_2 and stored at -80°C. All solutions contained the following protease inhibitors: phenylmethylsulfonyl fluoride (0.23 mM), soybean trypsin inhibitor (10 μg/ml), aprotinin (1.0 μg/ml), pepstatin A (1.0 μM), benzamidine (0.2 mM), and leupeptin (1.0 μM).

The optical bilayer system

The optical bilayer system used in the studies described in this and the accompanying report is schematized in Fig. 1. A small *trans* chamber was attached via a glass capillary tube to the head stage of an Axopatch 1-B patch clamp amplifier (Axon Instruments, Union City, CA) using a microelectrode holder (E.W. Wright, Guilford, CT). The head stage was, in turn, mounted on a 3-axis hydraulic manipulator (Narashige, East Meadow, NY), which was used to position the *trans* chamber within the *cis* chamber. A water immersion microscope objective (70×, 1.2 NA, Lomo Optics, Germantown,

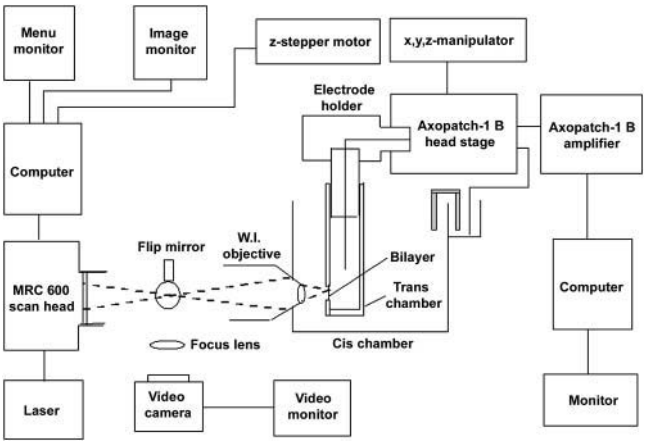

FIGURE 1 Components of the optical bilayer system. A schematic illustrating the components of an optical bilayer system capable of simultaneous measurement of fluorescence and electrical currents is shown. Fluo-3 fluorescence is imaged using a Bio-Rad MRC 600 confocal system, a water immersion (*WI*) objective (70×, NA 1.2), and an argon ion laser. The *trans* chamber is attached via a 2-mm glass capillary tube and an electrode holder to the head stage of a patch-clamp amplifier. The head stage is mounted on a 3-axis translation stage controlled by a hydraulic manipulator. Front-to-back movements of the *trans* chamber relative to the objective, which is fixed horizontally in the *cis* chamber, are used for focusing. The latter movements are imposed using a computer-controlled stepper motor. See text for additional details.

MD) was introduced in a horizontal orientation through the front wall of the *cis* chamber. Focusing was achieved by using a computer-driven stepper motor to adjust the position of the *trans* chamber relative to the objective. A small magnetic stir motor (not shown) was mounted in the rear wall of the *cis* chamber, where it held a small stir bar used to mix the contents of the *cis* chamber.

Construction of the *trans* chamber, and in particular restricting the depth of the hole across which the bilayer is painted is a critical step for successful imaging of the bilayer. As shown in the cartoon in panel *A* of Fig. 2, the beam emerging from a high numerical aperture objective, which goes from a clear aperture with millimeter dimensions to a diffraction limited spot over the working distance of the objective (~160 μm), exhibits a steep profile. As a consequence, the portion of the bilayer that can be scanned without interruption of the beam by the edges of the front wall of the *trans* chamber decreases rapidly with distance from the front of the chamber. An estimate of the maximal depth compatible with uninterrupted scanning of a bilayer with our optical system is shown in panel *B* of Fig. 2. A fluorescent solution was placed in both the *cis* and *trans* chambers in the absence of a bilayer. As the plane of focus was advanced into the hole that normally contained the bilayer the imaged fluorescence intensity remained constant until a depth of ~18 μm was reached. Beyond this point the fluorescence intensity declined rapidly indicating that the volume of fluorophore-containing solution being sampled was diminished. Since bilayers frequently form as far away from the front surface of the *trans* chamber as possible, it was necessary to use holes <15 μm deep. To meet this requirement, holes 50–100 μm in diameter were formed in small rectangular pieces of 12.5 μm thick Halar film. As shown in Fig. 3, the entire bilayer can be scanned when holes limited to this depth are used. The bilayer was imaged using reflected red (633 nm) light and a fluo-3 excitation/emission filter/dichroic beam splitter set. This arrangement permits imaging of the bilayer surface, as well as the ability to determine the distance between the bilayer and the front surface of the *trans* chamber. The latter information is necessary for analysis of how variations in the distance between the plane of focus and the plane of the RyR channel influence spark properties.

Fluorescence was imaged using a Bio-Rad MRC 600 confocal system mounted horizontally on an optical bench. Light at 488 nm from an argon ion laser was coupled into the system through a single-mode optical fiber. The *trans* chamber could also be illuminated obliquely with white light from an optical fiber bundle (not shown in Fig. 1) introduced through the rear sidewall of the *cis* chamber to generate a transmitted light image for initial

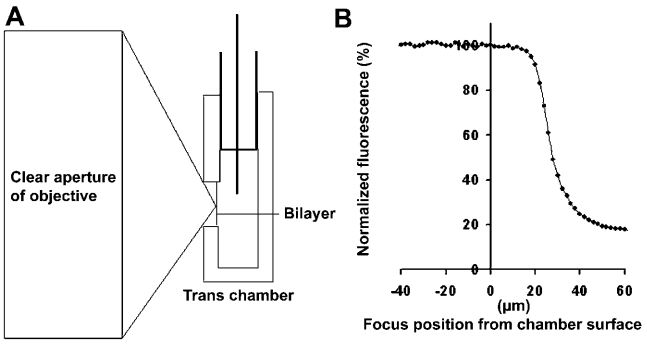

FIGURE 2 Geometric considerations for optical imaging of planar lipid bilayers. The distance between the plane of the bilayer and the front surface of the *trans* chamber impacts optical measurements. The profile of the laser beam focused by a 70× high NA objective is cartooned in panel *A*. Due to its profile, the beam cannot be scanned very deeply into the hole without being scattered by the edges of the hole. This scattering causes a loss of signal intensity from a uniformly distributed fluorescent solution as the plane of focus is moved into the hole (*panel B*). To ensure that the entire surface of the bilayer is scanned (see Fig. 3), it is necessary to make the thickness of the *trans*-chamber wall 15 μm or less.

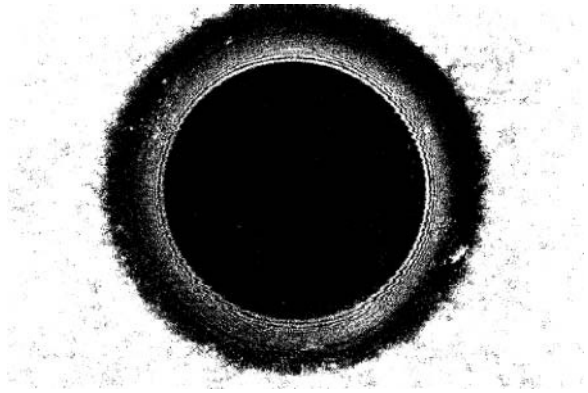

FIGURE 3 Locating the bilayer. Bilayers are imaged using reflected 633-nm light to establish their location relative to the front surface of the *trans* chamber. A bilayer formed in a 100-μm diameter hole is shown in this image. The bilayer is the black inner circle and is ~70 μm in diameter. The torus around the bilayer is shown by the white interference pattern and outer black region. The edge of the hole is the black to white transition. The depth of the bilayer in the hole is measured as the distance between the bilayer focal plane and the front surface of the *trans* chamber.

focusing of the *trans* chamber. The image is acquired by diverting light from the Bio-Rad system to a CCD camera parfocal with the Bio-Rad system with a flip-mount mirror. The output of the camera was viewed on a TV monitor. After initial positioning, reflected light images of the bilayer obtained with the Bio-Rad system were used to fine-focus on the plane of the bilayer (Fig. 3). Scanning and image acquisition were controlled using Comos software (Bio-Rad). Image export and processing were accomplished using Confocal Assistant software (developed by Todd Clark Brelje) and Adobe PhotoShop (version 7.0). The *x,y* images presented in this report contain 768 × 512 pixels (0.14 μm/pixel) and required ~1 s to acquire. The *x-t* line scans shown in Figs. 4 and 8 contain 512 lines and again required ~1 s to acquire.

Single channel recording

Bilayers were formed by painting using a solution containing either phosphatidylethanolamine (PE) or PE + phosphatidylserine (80:20) at a total lipid concentration of 25 mg/ml in decane. Initially, the *cis* chamber solution contained 85 mM Tris/Hepes, pH 7.4, and contaminating levels of free Ca^{2+} (2–10 μM, measured with Ca^{2+}-selective minielectrodes; McKemy et al., 2000), suitable for activating RyR2 channels. The *trans* chamber solution contained 50 mM $CaCl_2$ and 10 mM Tris/Hepes, pH 7.4. In the experiments described in Figs. 8 and 9, 2 μM annexin 12 was added to the *trans* chamber to restrict lateral diffusion of the RyR2 channel (see Peng et al., 2004, for details). Liposomes containing RyR2 channels were added to the *cis* chamber and fusion with the bilayer was enhanced by creation of an osmotic gradient by addition of 3M KCl to the *cis* chamber. After fusion occurred, the *cis* chamber was perfused while stirring with 5 vol of a solution containing 85 mM Tris/Hepes, pH 7.4. When perfusion was complete a final concentration of 25–75 μM fluo-3 was added to the *cis* chamber. Trans-bilayer currents were recorded and analyzed using a system comprised of an Axopatch 1B patch clamp amplifier, a Digidata 1200 interface, a PC computer, and pClamp 8 software.

The level of free Ca^{2+} in the *cis* chamber was buffered to 0.1 μM by addition of Chelex resin. Use of Chelex as a buffer was convenient for these initial studies for two reasons. Chelex sets the free Ca^{2+} concentration to 0.1 μM, a level compatible with maximal activation of RyR2 channels by suramin (see below). In addition, buffering in the vicinity of the bilayer occurred only when Chelex beads were stirred into the volume of the *cis* chamber. The beads settled back to the floor of the chamber when stirring

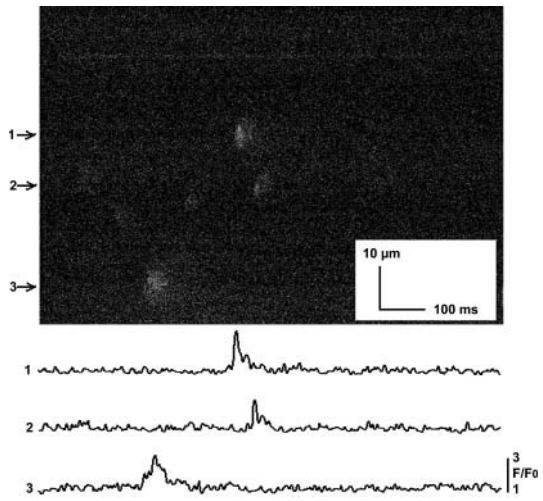

FIGURE 4 Sparks imaged in intact mouse cardiomyocytes with the optical bilayer system. A *x-t* line scan image of sparks in an intact ventricular cardiomyocyte bathed in 1 mM Ca^{2+} is shown. Myocytes were permitted to settle onto laminin-coated coverslips, which were fixed to the surface of the *trans* chamber in place of the bilayer partition. The *trans* chamber was positioned as for a bilayer experiment and the optical system was identical to that used to image Ca^{2+} fluxes across the bilayer. Intensity-time traces for the sparks numbered as indicated on the left side of the image are shown in the lower part of the figure. Cumulative data for the properties of sparks imaged in intact myocytes are presented in Table 1.

was stopped. This permitted baseline fluo-3 signals to be obtained with minimal Ca^{2+} buffering, although still allowing the level of free Ca^{2+} in the *cis* chamber to be reset to 0.1 μM during the course of an experiment. One application of the optical bilayer system will be to investigate influences of Ca^{2+} buffers on fluo-3 fluorescence. Therefore, it is important initially to obtain control fluorescent signals in the absence of significant Ca^{2+} buffering. Ca^{2+} and Tris ions are the only charge carriers available in the solutions used in the present studies and since sheep heart RyR2 channels have a Ca^{2+}/Tris permeability ratio of 15.3 (Lindsay and Williams, 1991) >99% of the *trans-cis* current will be carried by Ca^{2+}, as calculated using the model described by Tinker et al. (1993) (Alan Williams, personal communication).

A voltage command (VC) protocol was developed that permitted Ca^{2+} flux through RyR2 channels to be determined solely by the voltage imposed across the bilayer. Using this protocol, the amplitude, time course, shape, and consequently the magnitude, of the Ca^{2+} flux can be controlled with precision. To achieve such control, the open probability (P_o) of RyR2 channels must be maintained at, or close to, 1.0 during the voltage step, so Ca^{2+} fluxes are not affected by channel gating. To keep background fluo-3 fluorescence at acceptably low levels, it was also necessary to achieve this level of activation in the presence of submicromolar concentrations of free Ca^{2+} in the *cis* chamber. Based on the findings of Sitsapesan and Williams (1996) and Sitsapesan (1999) these requirements were met by addition of suramin (100–200 μM) to the *cis* chamber in the presence of 0.1 μM free Ca^{2+}. To prevent leak of Ca^{2+} through suramin-activated RyR2 channels, the *trans*-bilayer voltage was maintained at the reversal potential for RyR2 channel-mediated Ca^{2+} currents, typically −60 mV (*trans* relative to *cis*) between measurements. A comparable reversal potential was calculated using the model of Tinker et al. (1993) (Alan Williams, personal communication). The voltage was stepped to more positive *trans* voltages to elicit a net *trans*-to-*cis* Ca^{2+} flux. Using the VC protocol, reproducible Ca^{2+} fluxes and associated fluo-3 fluorescence responses could be achieved in a repetitive manner. Negative controls demonstrating the absence of fluo-3 fluorescence when there was no *trans*-to-*cis* Ca^{2+} current were obtained 1), from records where channels either failed to open at all or closed for a significant period during a step to positive voltages; 2), when the applied voltage was maintained at the reversal potential; and 3), when steps to voltages more negative than the holding potential were applied.

Isolation of ventricular cardiomyocytes from adult mice

Myocytes were isolated using standard techniques (Duan et al., 1999), permitted to recover to a Ca^{2+}-tolerant state, and loaded with the Ca^{2+} indicator, fluo-3 AM, using methods described by Ritter and co-workers (2000). Myocytes were permitted to settle onto cover slips coated with either polylysine or laminin, and the coverslips were fixed to the front wall of the *trans* chamber in an orientation identical to that of the lipid bilayer. Fluorescence imaging was then performed utilizing the same illumination, optics, and detection system used when a bilayer was present. In some experiments extracellular K^+ was elevated to 10−20 mM to increase the frequency of spontaneously occurring sparks.

RESULTS

Imaging of Ca^{2+} sparks in intact cardiomyocytes

A rationale underlying the design of the optical bilayer was to develop an in vitro system capable of analyzing the influences exerted by factors and conditions extrinsic to RyR channels on Ca^{2+} sparks imaged in intact cells. Consequently, it was necessary to demonstrate that cellular Ca^{2+} sparks imaged with the optical bilayer system had properties comparable to sparks reported by other laboratories using conventional microscope-based systems, or that our system could measure the event it was designed to study. Images of spontaneous Ca^{2+} sparks typical of those obtained from five separate myocyte isolations are shown in Fig. 4, and cumulative data describing spark properties are presented in Table 1. The values obtained for spark amplitude (F/F_o), rise time, full duration at half-maximum (FDHM) and full width at half-maximum (FWHM) are similar to those reported in the literature for ventricular cardiomyocytes from adult mice (e.g., Ritter et al., 2000) and comparable to those observed for sparks imaged in cardiomyocytes from other species (see compilation in Table 1 of Rios and Brum, 2002).

TABLE 1 Properties of spontaneous sparks imaged in isolated mouse ventricular cardiomyocytes using the optical bilayer system

	F/F_0	Rise time (ms)	FDHM (ms)	FNHM (μm)
Mean	2.52	10.97	34.53	2.79
SD	0.21	1.40	8.38	0.68

F/F_0, amplitude.
Rise time, time required for fluorescence to rise from 10 to 90% of maximum amplitude.
FDHM, full duration at half-maximum.
FWHM, full width at half-maximum.
Values were obtained from *x-t* line scans and data points were obtained by averaging values from five lines centered on the spark. $N = 42$ sparks imaged in 30 cells obtained from five different isolations.

Imaging Ca^{2+} flux through single RyR2 channels in bilayers

Examples of *x,y* images of fluo-3 fluorescent responses to Ca^{2+} flux through single RyR2 channels elicited with the VC protocol obtained in three separate experiments are shown in Fig. 5. The voltage across the bilayer was stepped from the reversal potential for *trans*-to-*cis* Ca^{2+} flux to a positive potential (*trans* relative to *cis*) just before scanning was initiated to elicit a continuous net Ca^{2+} flux into the *cis* chamber while images were obtained. Single RyR2 channel currents recorded simultaneously with fluorescence are shown in the insets in panels *A–C* of the figure. Capacitance transients are not seen in the traces, since they occurred before the start of the scan. The image in panel *A* may appear slightly asymmetric due to the location of the RyR2 channel at the left side of the bilayer near the region of the torus. In the experiment shown in panel *C*, the RyR2 channel closed for ~30 ms and then reopened while the position of the channel was being scanned. Because the *x,y* scan was acquired left to right from top to bottom, this resulted in bifurcation of the fluorescence signal. An intensity-time trace obtained from top to bottom through the center of the spark (*white vertical line* in *panel C*) is aligned with the current trace in panel *D*. The sharp demarcation of the period of channel closure, as well as the ramp responses shown in Fig. 8, and the *x-t* images shown in Fig. 5 in Peng et al. (2004) illustrate the kinetic properties of the optical system to changes in Ca^{2+} in the vicinity of the bilayer.

The effects of ryanodine (10 μM) and ruthenium red (10 μM) were assessed to confirm that both fluo-3 fluorescence and the single channel currents were due to Ca^{2+} flux through RyR2 channels. As shown in Fig. 6, changes produced by both agents are consistent with their well-established actions on RyR2 channels. Exposure to ryanodine, which produced a long-lived RyR2 channel subconductance state, resulted in appropriate reductions in both fluo-3 fluorescence and single channel current. Exposure to ruthenium red, a RyR2 channel blocker, eliminated both fluorescence and current. Closure of the channel in the control current trace did not result in bifurcation of the fluorescence (as in *panel C* of Fig. 5), since it occurred well after the position of the RyR2 channel in the bilayer had been scanned.

Estimates of the SR Ca^{2+} release flux that gives rise to Ca^{2+} sparks in cardiomyocytes suggest the involvement of a variable number of RyR2 channels. Thus, to mimic these events, it is necessary to produce a range of Ca^{2+} flux values in the bilayer system. Therefore, we investigated the relationship between the amplitude of the Ca^{2+} flux through single RyR2 channels and the associated change in fluo-3 fluorescence using the VC protocol. As described in the Methods section, with this protocol the magnitude of Ca^{2+} flux through a RyR2 channel is determined solely by the voltage gradient imposed across the bilayer. A range of amplitudes of Ca^{2+} flux through RyR2 channels was obtained by stepping to different *trans* relative to *cis* (positive) voltages. After normalization for baseline values, fluo-3 fluorescent intensity was proportional to the measured amplitude of Ca^{2+} flux through the RyR2 channel over the range of 0.25–14 pA (Fig. 7). The unitary RyR2 channel Ca^{2+} conductance under physiological conditions has been estimated to be ~0.5–1.4 pA (Mejia-Alvarez et al., 1999; Tinker et al., 1993). These studies used luminal Ca^{2+} concentrations of 1–10 mM. With these estimates, the range of RyR2 channel current amplitude in Fig. 7 is equivalent to the flux of Ca^{2+} through 1 to >20 RyR2 channels. Ca^{2+} flux is expressed as peak amplitude rather than as the total or cumulative net flux of Ca^{2+} obtained by integrating the current amplitude over the duration of the voltage step in this

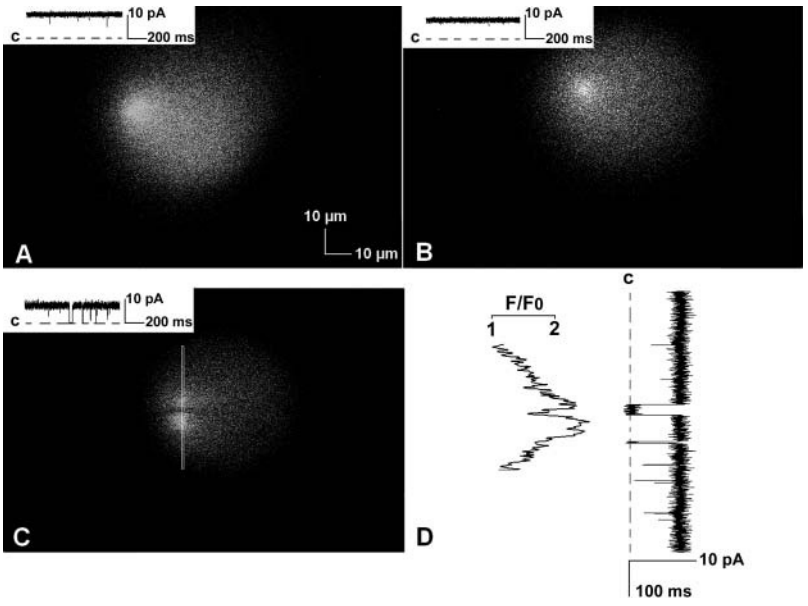

FIGURE 5 Bilayer "Ca^{2+} sparks." Three examples of fluo-3 fluorescence recorded in response to Ca^{2+} flux through single RyR2 channels reconstituted in bilayers are shown in panels *A–C*. These images contain 768 × 512 pixels (0.12 μm/pixel) and required 1 s to acquire (the scanning pattern was left to right, then top to bottom). Simultaneous recordings of single RyR2 channel currents are shown in the inset in each panel, where "C" indicates the level of zero net current. The dark horizontal zone through the bright center of the fluorescence signal in panel *C* resulted from a brief closing of the channel while the position of the channel was being scanned. An intensity versus time trace obtained from top to bottom through the center of the fluorescence (*white vertical line* in *panel C*) is aligned with the current trace in panel *D*. The conditions used in these experiments resulted in current amplitudes of 8–10 pA. The illuminated areas approximate the dimensions of the hole containing the bilayers. Background fluorescence is due to buildup of Ca^{2+} in the *cis* chamber with repeated voltage steps.

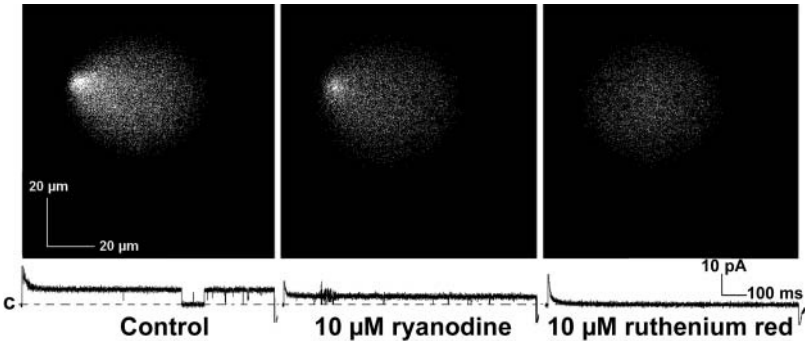

FIGURE 6 Fluo-3 fluorescence and Ca^{2+} currents are the result of Ca^{2+} flux through RyR2 channels. Fluo-3 fluorescence and RyR2 Ca^{2+} currents are reduced by 10 μM ryanodine to subconductance state levels (*middle panel*) and abolished by 10 μM ruthenium red (*right panel*). Both ryanodine and ruthenium red were added to the *cis* chamber. The capacitance transients associated with the current traces were reduced graphically by ~50% during figure preparation. "C" indicates the level of zero current. These data confirm that both the fluorescence and the currents are due to Ca^{2+} flux through a RyR2 channel.

figure. Since the same duration was used for all voltage steps and P_o ~1.0, integration resulted in only a proportional shift of the values and did not alter qualitative aspects of the relationship between fluorescence and Ca^{2+} flux.

As noted in the Introduction, RyR2 channels in a CRU may activate in a coordinated manner. In this case, RyR2 channels mediating the Ca^{2+} flux responsible for a Ca^{2+} spark could activate and inactivate at the same time and this type of activity could be mimicked as a square step in RyR2 channel Ca^{2+} current, similar to that shown in Fig. 5 of the accompanying report. Alternatively, individual RyR2 channels could activate and inactivate at different rates and a more complex current waveform would be required to simulate this type of activity. For example, fluo-3 fluorescence elicited by ramping rather than stepping the *trans*-bilayer voltage is shown in Fig. 8. The ramp protocol produces a rise and fall in fluo-3 fluorescence, which in some cases may be more similar to the rising phase of sparks imaged in cardiomyocytes. The ability to elicit arbitrarily complex Ca^{2+} flux waveforms demonstrates further the ability of the VC protocol to mimic aspects of the relationships between optical recordings and the flux of Ca^{2+} through RyR2 channels in cells. The change in fluorescence intensity shown in this figure is in good agreement temporally with the imposed change in voltage, again illustrating the temporal properties of the optical bilayer system.

To simplify initial studies, purified RyR2 channels were reconstituted in liposomes at a low protein/lipid ratio to enhance incorporation of single channels. However, on occasion RyR2 channel Ca^{2+} currents that were multiples of the unitary current were recorded indicating the presence of more than one active RyR2 channel in the bilayer. As shown in the *x*,*y* images presented in Fig. 9, when this occurred multiple foci of fluo-3 fluorescence were imaged. In the experiment shown in the upper left panel of the figure, one of two RyR2 channels did not open until its position in the

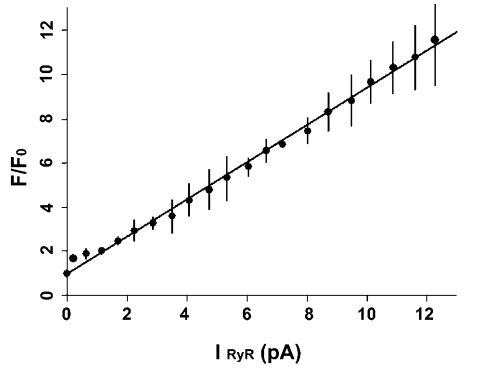

FIGURE 7 Fluo-3 fluorescence is proportional to the Ca^{2+} flux through a RyR2 channel. Ca^{2+} currents with different amplitudes were generated using the VC protocol. Fluo-3 fluorescence signals increased proportionally in response to Ca^{2+} current amplitudes of 0.25–12 pA.

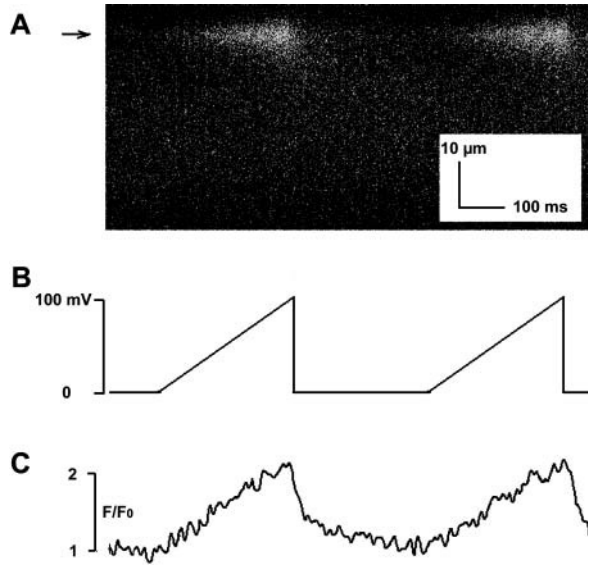

FIGURE 8 The VC protocol can be used to produce Ca^{2+} fluxes having arbitrarily complex waveforms. A *x-t* line scan image of fluo-3 fluorescence in response to Ca^{2+} fluxes through a single RyR2 channel (*panel A*) were elicited in the bilayer system using voltage ramps (*panel B*). Fluorescence intensity-time traces obtained at the location indicated by the arrow in panel *A* are shown in panel *C*. As in Table 1, values were obtained by averaging data from five lines centered on the spark. These data illustrate the capability of the VC protocol to mimic different rates of activation and inactivation of clusters of multiple RyR2 channels. In addition, the temporal similarity between the voltage command signal and the imaged fluorescence demonstrate the temporal properties of the optical bilayer system.

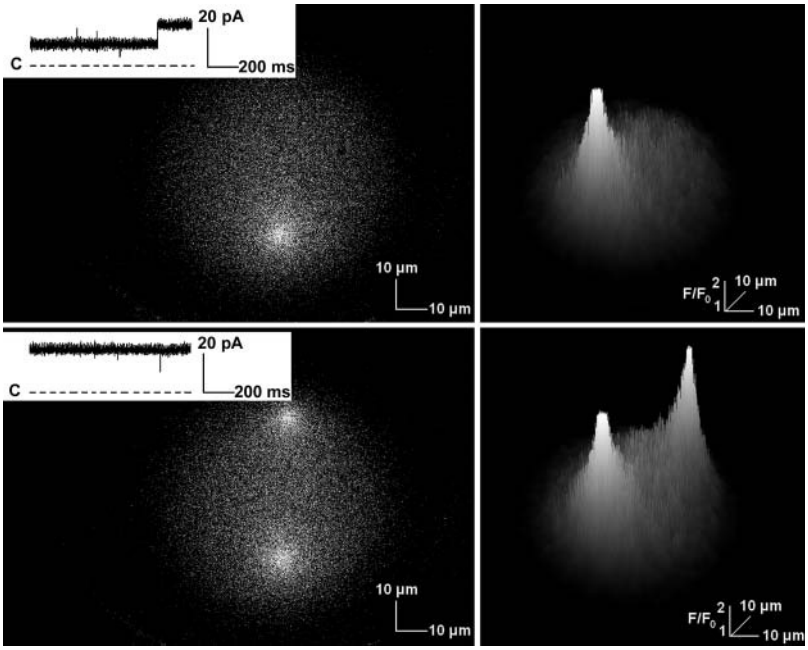

FIGURE 9 Ca^{2+} flux through multiple RyR2 channels imaged in the bilayer system. A single RyR2 channel was active during most of the 1-s *x*,*y* scan shown in the top left panel. A second RyR2 channel activated toward the end of the scan, but only a single fluorescent signal was observed since this channel was in a region of the bilayer that had already been imaged. Both RyR2 channels were active during the entirety of a subsequent scan (*bottom left panel*) and two discrete fluorescent signals were recorded. RyR2 Ca^{2+} currents recorded during the scans are shown in the insets of these panels. Three-dimensional representations of the associated intensity changes are shown in the panels on the right side of the figure. The flattened tops of the signals result from the square shape of the Ca^{2+} flux and not from signal saturation.

bilayer had already been scanned. Consequently, only a single fluorescence signal was observed. During the next scan shown in the lower left panel, both RyR2 channels activated and two fluorescence signals were imaged. Three-dimensional representations of the *x*,*y* images are presented in the panels on the right side of the figure. Inspection of the intensity values indicated that the flattened tops of the signals are due to the square shape of the fluorescence signal and not to signal saturation. Another example of this shape can be seen in the intensity-time traces shown in Fig. 5 in Peng et al. (2004). These data demonstrate further the ability to establish the location of active RyR channels using the optical bilayer system.

DISCUSSION

In this article, we describe development of an optical bilayer system and demonstrate its utility for simultaneous fluorescent imaging and electrical recording of Ca^{2+} fluxes through single RyR2 channels. In Peng et al. (2004), we describe use of this system to characterize lateral diffusion of RyR2 channels in bilayers and identification of the ability of annexin 12 to effectively immobilize RyR2 channels within the bilayer. Below, we discuss additional technical aspects of the bilayer system and application of this system to three areas of current research.

Additional considerations concerning the optical bilayer system

The optical bilayer system can be used with both widefield (nonscanned) and laser scanning confocal fluorescence imaging systems (LSCS). We implemented a LSCS for three reasons. First, as discussed below, a motivation for developing an optical bilayer system was to provide a complementary approach for characterizing the relationships between Ca^{2+} indicator fluorescence and the flux of Ca^{2+} through RyR2 channels. LSCS have been used in the majority of studies in the literature that describe properties of Ca^{2+} sparks imaged in cells. Therefore, we felt it was necessary to use a similar imaging system to make meaningful comparisons between reported data and results obtained with the bilayer system.

Second, LSCS image fluorescence in a restricted volume. This ability is important for the temporal resolution observed for fluorescence imaged in the optical bilayer system. As shown in Figs. 4 and 9 of this report and Fig. 5 of Peng et al. (2004), the temporal and dynamic resolution of fluo-3 fluorescence tracks elicited Ca^{2+} fluxes in a reasonable manner. The rapidity of the diffusion of Ca^{2+} from the restricted volume being imaged is one reason for the temporal resolution achievable with the optical bilayer system. Future studies will address the extent to which the on- and off-rates of the indicator-Ca^{2+} binding reaction and rebinding of Ca^{2+} during a single Ca^{2+} flux event contribute to the time course observed for the fluorescent responses.

A third reason for use of a LSCS was to utilize detectors with the greatest data acquisition rates. Currently, single point detectors, such as photodiodes and photomultiplier tubes, have greater sampling rates than detector arrays, such as CCD cameras, typically used with nonscanned widefield systems. The ability to immobilize RyR2 channels in the bilayer described in the accompanying report will permit parking the laser beam on the position of the channel and

recording fluorescence with photon-limited temporal resolution.

A potential complicating factor associated with the optical bilayer system is that under certain conditions the structure and properties of the bilayer may influence fluorescence responses to Ca^{2+} fluxes. Several factors may create asymmetry in the fluorescent signal. These include an illusion of asymmetry when a channel is located at the edge of the bilayer, resulting in greater intensity values on one side of the channel, particularly as background Ca^{2+} levels are increased by RyR2 channel activity. For example, this can be appreciated by comparing the bilayer fluorescence signals shown in panels *A* and *B* in Fig. 5. Second, curvature of the bilayer as it approaches the torus can produce spatial aberrations. Third, care must be taken to ensure that the face of the objective is parallel with the plane of the bilayer. Properties of the optical system may also contribute to signal asymmetry. As bearing surfaces in scan mirror galvanometers age, they can become nonlinear and result in distorted spatial representations. Also, depending on their design, microscope objectives have varying degrees of spherical aberration.

Application of the optical bilayer system to areas of current research

Analysis of Ca^{2+} sparks

Ca^{2+} sparks offer unique insights into cellular activation and the function of RyR2 Ca^{2+} release channels in intact cells. A rigorous analysis of RyR2 channel activity in situ requires accurate estimates of the magnitude of the Ca^{2+} flux through single RyR2 channels, the total quantity or mass of Ca^{2+} underlying a spark, and the temporal properties of the Ca^{2+} flux. However these estimates are difficult to make, since the waveform of the spark is distorted from that of the underlying Ca^{2+} flux by cellular factors extrinsic to RyR2 channels. These factors include concerted gating of multiple RyR2 channels, diffusion of free Ca^{2+} and Ca^{2+} bound to mobile buffers, the kinetics of Ca^{2+} binding to the Ca^{2+} indicator, the extent of binding of the Ca^{2+} indicator to cellular proteins, release of Ca^{2+} into a restricted space, competition for Ca^{2+} with removal processes, and having the plane of focus distant from the site of Ca^{2+} release. The optical bilayer system can be used to compare cellular sparks with bilayer sparks obtained in response to a known range of Ca^{2+} fluxes elicited with the VC protocol that encompass those thought to occur in intact cardiomyocytes. As shown in Fig. 4, it is possible to compare bilayer sparks with cellular Ca^{2+} sparks imaged with the same optical system.

Two approaches have been used to measure the Ca^{2+} flux underlying sparks imaged in cardiac myocytes. In technically elegant experiments, Wang et al. (2001) used fluo-4 fluorescence responses to Ca^{2+} fluxes through voltage-gated L-type Ca^{2+} channels to calibrate the Ca^{2+} flux underlying Ca^{2+} sparks measured in the same rat ventricular myocyte and estimated that a spark involves ~2.1 pA of Ca^{2+} flux (also see Cheng and Wang, 2002). As noted in the Introduction, others have used simulation and modeling to account for influences of factors, such as those discussed in the preceding paragraph, and estimate the Ca^{2+} flux underlying a spark. In general, estimates of Ca^{2+} fluxes associated with sparks obtained by modeling exceed that of Wang et al. (2001). For example, Soeller and Cannell (2002) concluded that sparks imaged in rat ventricular cardiomyocytes involve a Ca flux >7.5 pA. Both imaging and modeling approaches should yield similar estimates of the Ca^{2+} flux underlying a spark, and as noted by Rios and Brum (2002), discrepancies between these estimates may in part be due to systematic selection of different size sparks by the different laboratories. However, Baylor et al. (2002) demonstrated recently that the accuracy of simulations of Ca^{2+} sparks imaged in frog skeletal muscle fibers is greatly enhanced by improved estimates of Ca^{2+} binding to cellular proteins and the properties of Ca^{2+} binding to the Ca^{2+} indicator, fluo-3, and by maximizing the spatial resolution of the optical system. This work indicates the importance of a more complete understanding of the effects of cellular factors on the spatial and temporal properties of Ca^{2+} sparks. Consequently, a rationale for development of the optical bilayer was to provide a system suitable for a bottom-up assessment of their impact on the properties of a ''spark'' waveform in a direct and systematic manner.

The VC protocol is an important component in our approach. Setting the P_o of a RyR2 channel to ~1.0 permits precise control over the amplitude, time course, and shape of Ca^{2+} fluxes through single RyR2 channels. Since RyR2 channel currents are measured, any occasional deviations from a unitary P_o are taken into account. The ability to control Ca^{2+} flux allows systematic variation of its magnitude and time course and ranges of values for parameters of RyR channel function to be investigated. This avoids bias and assumptions about the values of RyR2 channel parameters in intact cells, where little is known with certainty. Ca^{2+} sparks are generally accepted to be the product of Ca^{2+} flux through multiple RyR2 channels localized in a CRU. Using the estimates of unitary physiological RyR2 channel Ca^{2+} conductance by Tinker et al. (1993) and Mejia-Alvarez et al. (1999), the range of RyR2 channel Ca^{2+} current amplitudes achievable with saturating levels of *trans* Ca^{2+} in the optical bilayer system is sufficient to mimic unitary Ca^{2+} currents through ~1 to >20 RyR2 channels. Moreover, as shown in Fig. 9, voltage ramps can be used to vary the steepness and shape of the rising and falling phases of the command signal to mimic nonhomogeneities in the rates of activation and/or inactivation of individual RyR2 channels within a CRU. The ability to immobilize RyR2 channels in bilayers described in Peng et al. (2004) makes it possible to use *x-t* or line scans through the position of the functional RyR2 channel for

repetitive analysis of Ca^{2+} indicator responses to measured Ca^{2+} fluxes. The reproducible nature of the fluorescence signals to consecutive voltage steps (see Fig. 8 in this report, and Fig. 5 of Peng et al., 2004) make it possible to use signal averaging to improve signal-to-noise.

Coupled gating of RyR channels

Analysis of the mechanism(s) underlying coupled gating of RyR channels may also benefit from application of the optical bilayer system. Studies by Marx et al. (1998, 2001) indicate that multiple RyR channels in bilayers can exhibit coupled gating. Exposure to rapamycin, which causes FK506 binding proteins (FKBP) to dissociate from RyR channels, resulted in non-coordinated gating and it was suggested that coordination of gating may involve interactions between adjacent RyR channels stabilized by binding of FKBP to RyR. Activation of RyR channels by the Ca^{2+}-induced Ca^{2+} release (CICR) mechanism (Fabiato and Fabiato, 1975) could provide an alternative or additional mechanism for coordinating activation of closely grouped RyR channels (Copello et al., 2003). In this case, Ca^{2+} released from one RyR channel would activate one or more nearby RyR channels in a sequential or parallel manner. The CICR mechanism would not require physical contact between RyR and may permit coordination of RyR channels separated by greater distances. The optical bilayer system may help to distinguish between these mechanisms. If distances between RyR channels coordinated by CICR are sufficiently great, it will be possible to resolve Ca^{2+} indicator signals having multiple peak amplitudes. The centroid of each peak can be determined to yield estimates of inter-RyR channel distances. Since the molecular dimensions of RyR channels are known (Wagenknecht and Samso, 2002), it should be possible to decide whether these distances are compatible with physical contact between RyR channels.

Structure-function relationships of RyR channels

A long-term goal for development of an optical bilayer system is to provide one of the tools required for analyses of the changes in RyR channel structure responsible for channel function. Significant steps have been made toward providing the other tools required for such experiments. As discussed in the Introduction, the relationship between the primary sequence and the tertiary structure of RyR channels is being elucidated using cryoelectron microscopy. Although not capable of atomic resolution, this approach does provide an initial basis set of information. In addition, significant advances have been made in producing diffracting crystals of membrane proteins (Jiang et al., 2002, 2003; Nishida and MacKinnon, 2002). Studies of RyR channel structure-function relationships will be facilitated by the use of molecular modeling based on structural homology with other ion channels (Williams et al., 2001). New strategies for introducing reporter groups with conformation-dependent fluorescence signals into RyR channels in a site-directed manner will have to be developed; however, work by Ikemoto and coworkers who have recorded variations in fluorescence intensity from populations of labeled RyR channels during release of Ca^{2+} from SR vesicles (Ohkusa et al., 1991; Yamamoto and Ikemoto, 2002) supports the feasibility of this step. Finally, recent studies involving K^+ and gramicidin channels demonstrate the feasibility of recording channel conformation-dependent fluorescence signals from single ion channels (Borisenko et al., 2003; Sonnleitner et al., 2002).

The abilities to image fluorescence responses to single RyR2 channel Ca^{2+} currents and to immobilize RyR channels in bilayers described for the first time in this and the accompanying report will make important contributions to studies of single RyR channels. As noted in a preliminary report, not all fluorescently labeled channel proteins that associate with a bilayer reconstitute as functional ion channels (Blunck et al., 2003). This makes it necessary to distinguish fluorescence signals associated with active channels. This situation is confounded by the fact that many fluorophores emit light in an intermittent manner, which could be interpreted as a functionally related signal, but be derived from an inactive channel. To avoid this problem, it is essential to identify the ion channel(s) conducting the currents being recorded. The ability to image Ca^{2+} flux through single (or multiple) RyR channels demonstrated in this report provides a way to precisely locate the position of active RyR channel(s) in the bilayer.

In conclusion, we have developed an optical bilayer system capable of simultaneous imaging of Ca^{2+} flux through single RyR2 channels reconstituted in planar lipid bilayers and electrical recording of single channel currents. Capabilities of this system are demonstrated and its utility for addressing several current research problems is discussed.

The authors gratefully acknowledge helpful discussions with Bill Wonderlin concerning fabrication of small bilayer holes, Alan Williams on properties of RyR2 channels in bilayers, and Gil Weir on the properties of custom confocal systems. We also thank Alan for his assistance with calculating the reversal potential and estimating the percentage of the measured current carried by Ca^{2+}. JLS would like to acknowledge the extremely important input of Dr. Rebecca Sitsapesan during initial efforts to fabricate *trans* chambers suitable for optical recording and for suggesting use of suramin as a suitable activator of RyR2 channels. We also thank Alan Williams and Rebecca Sitsapesan for commenting on this report.

The authors of this report received support from the following sources: J.A.A., S.P., and J.L.S. from National Institutes of Health grants HL53677 and AR45112; N.G.P. and J.L.S. from a National Science Foundation EPSCoR grant EPS0132556: G.J.K. from the Canadian Institutes of Health Research and the Heart and Stroke Foundation of Alberta; and D.D. from National Institutes of Health grants HL63914 and NCRR P20 RR15581.

REFERENCES

Airey, J. A., C. F. Beck, K. Murakami, S. J. Tanksley, T. J. Deerinck, M. H. Ellisman, and J. L. Sutko. 1990. Identification and localization of two triad junctional foot protein isoforms in mature avian fast twitch skeletal muscle. *J. Biol. Chem.* 265:14187–14194.

Baylor, S. M., S. Hollingworth, and W. K. Chandler. 2002. Comparison of simulated and measured calcium sparks in intact skeletal muscle fibers of the frog. *J. Gen. Physiol.* 120:349–368.

Blunck, R., J. L. Vazquez-Ibar, Y.-S. Liu, E. Perozo, and F. Bezanilla. 2003. Fluorescence measurements of KcsA channels in artificial bilayers. *Biophys. J.* 84:124a. (Abstr.)

Borisenko, V., T. Lougheed, J. Hesse, E. Fureder-Kitzmuller, N. Fertig, J. C. Behrends, G. A. Woolley, and G. J. Schutz. 2003. Simultaneous optical and electrical recording of single gramicidin channels. *Biophys. J.* 84:612–622.

Cannell, M. B., and C. Soeller. 2002. A mode of thought in excitation-contraction coupling. *Biophys. J.* 83:1–2.

Cha, A., G. E. Snyder, P. R. Selvin, and F. Bezanilla. 1999. Atomic scale movement of the voltage-sensing region in a potassium channel measured via spectroscopy. *Nature.* 402:809–813.

Cheng, H., and S. Q. Wang. 2002. Calcium signaling between sarcolemmal calcium channels and ryanodine receptors in heart cells. *Front. Biosci.* 7:d1867–1878.

Cheng, H., W. J. Lederer, and M. B. Cannell. 1993. Calcium sparks: elementary events underlying excitation-contraction coupling in heart muscle. *Science.* 262:740–744.

Copello, J. A., M. Porta, P. Diaz-Silvester, A. Nani, A. L. Escobar, S. Fleischer, and M. Fill. 2003. ''Coordinated'' gating of multiple ryanodine receptor channels (RyRs). *Biophys. J.* 84:17a. (Abstr.)

Duan, D., L. Ye, F. Britton, L. J. Miller, J. Yamazaki, B. Horowitz, and J. R. Hume. 1999. Purinoceptor-coupled Cl- channels in mouse heart: a novel, alternative pathway for CFTR regulation. *J. Physiol.* 521:43–56.

Fabiato, A., and F. Fabiato. 1975. Contractions induced by a calcium-triggered release of calcium from the sarcoplasmic reticulum of single skinned cardiac cells. *J. Physiol.* 249:469–495.

Fill, M., and J. A. Copello. 2002. Ryanodine receptor calcium release channels. *Physiol. Rev.* 82:893–922.

Franzini-Armstrong, C., F. Protasi, and V. Ramesh. 1999. Shape, size, and distribution of Ca(2+) release units and couplons in skeletal and cardiac muscles. *Biophys. J.* 77:1528–1539.

Ikemoto, N., and T. Yamamoto. 2002. Regulation of calcium release by interdomain interaction within ryanodine receptors. *Front. Biosci.* 7:d671–683.

Izu, L. T., J. R. Mauban, C. W. Balke, and W. G. Wier. 2001. Large currents generate cardiac Ca2+ sparks. *Biophys. J.* 80:88–102.

Jiang, Y. H., M. G. Klein, and M. F. Schneider. 1999. Numerical simulation of Ca(2+) ''Sparks'' in skeletal muscle. *Biophys. J.* 77:2333–2357.

Jiang, Y., A. Lee, J. Chen, M. Cadene, B. T. Chait, and R. MacKinnon. 2002. Crystal structure and mechanism of a calcium-gated potassium channel. *Nature.* 417:515–522.

Jiang, Y., A. Lee, J. Chen, V. Ruta, M. Cadene, B. T. Chait, and R. MacKinnon. 2003. X-ray structure of a voltage-dependent K+ channel. *Nature.* 423:33–41.

Lindsay, A. R., and A. J. Williams. 1991. Functional characterisation of the ryanodine receptor purified from sheep cardiac muscle sarcoplasmic reticulum. *Biochim. Biophys. Acta.* 1064:89–102.

Liu, Z., J. Zhang, P. Li, S. R. Chen, and T. Wagenknecht. 2002. Three-dimensional reconstruction of the recombinant type 2 ryanodine receptor and localization of its divergent region 1. *J. Biol. Chem.* 277:46712–46719.

Marx, S. O., J. Gaburjakova, M. Gaburjakova, C. Henrikson, K. Ondrias, and A. R. Marks. 2001. Coupled gating between cardiac calcium release channels (ryanodine receptors). *Circ. Res.* 88:1151–1158.

Marx, S. O., K. Ondrias, and A. R. Marks. 1998. Coupled gating between individual skeletal muscle Ca2+ release channels (ryanodine receptors). *Science.* 281:818–821.

McKemy, D. D., W. Welch, J. A. Airey, and J. L. Sutko. 2000. Concentrations of caffeine greater than 20 mM increase the indo-1 fluorescence ratio in a Ca(2+)-independent manner. *Cell Calcium.* 27:117–124.

Mejia-Alvarez, R., C. Kettlun, E. Rios, M. Stern, and M. Fill. 1999. Unitary Ca2+ current through cardiac ryanodine receptor channels under quasi-physiological ionic conditions. *J. Gen. Physiol.* 113:177–186.

Nishida, M., and R. MacKinnon. 2002. Structural basis of inward rectification: cytoplasmic pore of the G protein-gated inward rectifier GIRK1 at 1.8 A resolution. *Cell.* 111:957–965.

Ohkusa, T., J. J. Kang, M. Morii, and N. Ikemoto. 1991. Conformational change of the foot protein of sarcoplasmic reticulum as an initial event of calcium release. *J. Biochem. (Tokyo).* 109:609–615.

Ondrias, K., and A. Mojzisova. 2002. Coupled gating between individual cardiac ryanodine calcium release channels. *Gen. Physiol. Biophys.* 21:73–84.

Peng, S., N. G. Publicover, J. A. Airey, J. E. Hall, H. T. Haigler, D. Jiang, S. R. W. Chen, and J. L. Sutko. 2004. Diffusion of single cardiac ryanodine receptors in lipid bilayers is decreased by annexin 12. *Biophys. J.* 86:145–151.

Peng, S., N. Publicover, G. Kargacin, J. Airey, and J. Sutko. 2003. Visualization of single ryanodine receptors (RyR) in bilayers. *Biophys. J.* 84:387a. (Abstr.)

Pratusevich, V. R., and C. W. Balke. 1996. Factors shaping the confocal image of the calcium spark in cardiac muscle cells. *Biophys. J.* 71:2942–2957.

Rios, E., and G. Brum. 2002. Ca2+ release flux underlying Ca2+ transients and Ca2+ sparks in skeletal muscle. *Front. Biosci.* 7:d1195–1211.

Ritter, M., Z. Su, K. W. Spitzer, H. Ishida, and W. H. Barry. 2000. Caffeine-induced Ca(2+) sparks in mouse ventricular myocytes. *Am. J. Physiol. Heart Circ. Physiol.* 278:H666–H669.

Serysheva, I. I., M. Schatz, M. van Heel, W. Chiu, and S. L. Hamilton. 1999. Structure of the skeletal muscle calcium release channel activated with Ca2+ and AMP-PCP. *Biophys. J.* 77:1936–1944.

Sitsapesan, R. 1999. Similarities in the effects of DIDS, DBDS and suramin on cardiac ryanodine receptor function. *J. Membr. Biol.* 168:159–168.

Sitsapesan, R., and A. J. Williams. 1990. Mechanisms of caffeine activation of single calcium-release channels of sheep cardiac sarcoplasmic reticulum. *J. Physiol.* 423:425–439.

Sitsapesan, R., and A. J. Williams. 1994. Gating of the native and purified cardiac SR Ca(2+)-release channel with monovalent cations as permeant species. *Biophys. J.* 67:1484–1494.

Sitsapesan, R., and A. J. Williams. 1996. Modification of the conductance and gating properties of ryanodine receptors by suramin. *J. Membr. Biol.* 153:93–103.

Smith, G. D., J. E. Keizer, M. D. Stern, W. J. Lederer, and H. Cheng. 1998. A simple numerical model of calcium spark formation and detection in cardiac myocytes. *Biophys. J.* 75:15–32.

Smith, J. S., R. Coronado, and G. Meissner. 1986. Single-channel calcium and barium currents of large and small conductance from sarcoplasmic reticulum. *Biophys. J.* 50:921–928.

Sobie, E. A., K. W. Dilly, J. Dos Santos Cruz, W. J. Lederer, and M. S. Jafri. 2002. Termination of cardiac Ca(2+) sparks: an investigative mathematical model of calcium-induced calcium release. *Biophys. J.* 83:59–78.

Soeller, C., and M. B. Cannell. 2002. Estimation of the sarcoplasmic reticulum Ca2+ release flux underlying Ca2+ sparks. *Biophys. J.* 82: 2396–2414.

Sonnleitner, A., L. M. Mannuzzu, S. Terakawa, and E. Y. Isacoff. 2002. Structural rearrangements in single ion channels detected optically in living cells. *Proc. Natl. Acad. Sci. USA.* 99:12759–12764.

Tinker, A., A. R. Lindsay, and A. J. Williams. 1993. Cation conduction in the calcium release channel of the cardiac sarcoplasmic reticulum under physiological and pathophysiological conditions. *Cardiovasc. Res.* 27:1820–1825.

Vazquez-Ibar, J. L., A. B. Weinglass, and H. R. Kaback. 2002. Engineering a terbium-binding site into an integral membrane protein for luminescence energy transfer. *Proc. Natl. Acad. Sci. USA*. 99:3487–3492.

Wagenknecht, T., and M. Samso. 2002. Three-dimensional reconstruction of ryanodine receptors. *Front. Biosci.* 7:d1464–1474.

Wang, S. Q., L. S. Song, E. G. Lakatta, and H. Cheng. 2001. Ca2+ signalling between single L-type Ca2+ channels and ryanodine receptors in heart cells. *Nature*. 410:592–596.

Wang, S. Q., L. S. Song, L. Xu, G. Meissner, E. G. Lakatta, E. Rios, M. D. Stern, and H. Cheng. 2002. Thermodynamically irreversible gating of ryanodine receptors in situ revealed by stereotyped duration of release in Ca(2+) sparks. *Biophys. J.* 83:242–251.

Williams, A. J., D. J. West, and R. Sitsapesan. 2001. Light at the end of the Ca(2+)-release channel tunnel: structures and mechanisms involved in ion translocation in ryanodine receptor channels. *Q. Rev. Biophys.* 34:61–104.

Yamamoto, T., and N. Ikemoto. 2002. Peptide probe study of the critical regulatory domain of the cardiac ryanodine receptor. *Biochem. Biophys. Res. Commun.* 291:1102–1108.